Seismic Response of Bridges Accounting for Soil-Structure Interaction Effects and the Non-Synchronous Ground Motion due to 1D and 2D Site Analysis

Maria Chiara Capatti, Sandro Carbonari, Michele Morici
Department of Construction, Civil Engineering and Architecture. Via Brecce Bianche, 60131 Ancona, Italy

Francesca Dezi
Department of Economy, Science and Law. Via salita alla Rocca, 47890 San Marino, Rep. of San Marino

Graziano Leoni
School of Architecture and Design. Viale della Rimembranza, 63100 Ascoli Piceno, Italy

Francesco Silvestri
Dipartimento di Ingegneria Civile, Edile e Ambientale. Via Claudio 21, 80125 Napoli, Italy

Giuseppe Tropeano
Dipartimento di Ingegneria Civile, Ambientale e Architettura. Via Marengo 2, 09123 Cagliari, Italy

Keywords: Bridges; Soil-structure interaction; Site Response; Spatial variability; Substructure approach

ABSTRACT
This work focuses on the effects of soil-structure interaction and the spatial variability of seismic motion due to site effects on the seismic response of a multi-span viaduct on pile foundations. In particular, site effects induced in a soft clay deposit by an inclined bedrock layout are evaluated through different models, characterised by an increasing level of accuracy, which allows determining the free-field motion that is adopted to perform soil-structure interaction analyses in the frame of the substructure approach. The seismic input is represented at the outcropping bedrock by a set of suitably selected and scaled real accelerograms. After a brief presentation of the adopted numerical procedure, analyses results are presented focusing on both site and structural response. Amplifications effects obtained from simplified linear equivalent 1D and nonlinear 2D site response models are compared, discussing the applicability of the simplified approach. Structural responses, obtained by considering the non-synchronous motion resulting from the local stratigraphic conditions, in conjunction with soil-structure interaction effects, are shown in terms of piers displacement and ductility demands. Furthermore, the role of soil-structure interaction is clarified comparing results with those obtained from fixed base bridge models, proving that its contribution is more significant if the simplified model for site response is adopted.

1 INTRODUCTION

Seismic design of bridges is often performed neglecting Soil-Structure Interaction (SSI) effects and making the assumption that each support is subjected to the same input motion. However, SSI may sensibly affect the superstructure response to such an extent that it is impossible to a priori establish whether the effects are beneficial or detrimental with respect to individual structural components (Carbonari et al., 2011). Furthermore, previous researches (e.g. Monti et al., 1996; Lupoi et al., 2005) have demonstrated that, especially for long bridges, the spatial variability of ground motion may be responsible for significant additional forces and deformations in structural members.

The spatial variability of ground motion is usually attributed to three main factors: (*i*) the different arrival times of seismic waves at each site due to the finite propagation velocity (*wave-passage effect*); (*ii*) the loss of coherency induced by multiple refractions, reflections and interferences of the incident seismic waves and (*iii*) the different local soil conditions at each support of the bridge. In particular, the latter may be responsible of significant variation of the ground motion amplitude and frequency content between different supports. Moreover, the motion experienced by the foundation differs from the free-field motion and it is constituted by both translational and rotational components, as a consequence of kinematic interaction phenomena.

Dealing with the effect of spatial variability of ground motion on the seismic response of bridges, the above factors are often studied separately to capture contributions relevant to the structural response (e.g. Abrahamson et al., 1991; Monti et al., 1996). However, to the authors

knowledge, only the work by Sextos et al. (2003) include SSI in the analysis of multi-support bridges subjected to non-synchronous actions and thus further investigations are needed.

This work aims to investigate the effects of the non-synchronous ground motion induced by the variability of the local site amplification, on the seismic response of multi-span viaducts founded on piles, including SSI effects. A case study constituted by a multi-span bridge founded on a soft clay deposit overlaying an inclined bedrock is considered. The action is represented by real accelerograms defined at the outcropping bedrock and the spatial variation of ground motion for the bridge is evaluated by adopting different approaches to compute site amplification effects. In particular, several independent 1D linear equivalent analysis in correspondence of each bridge support and a 2D nonlinear model of the whole deposit are used to predict the stratigraphic amplifications to be used in the subsequent soil-structure interaction analyses.

SSI analyses of the bridge are performed according to the substructure approach, starting from the free-field motion obtained from the different models of the soil deposit. The kinematic interaction analysis of the soil-foundation system is formulated in the frequency domain by adopting the model of Dezi et al. (2009), while the inertial interaction analysis is carried out in the time domain to account for the non-linear structural behaviour. The frequency-dependent behaviour of the soil-foundation system is included through the Lumped Parameter Model (LPM) (Wolf, 1994).

The seismic response of the fixed-base and compliant base bridges, associated to the two site response models, are compared in terms of piers displacement and ductility demands. The contribution of SSI on the overall response is also addressed comparing results from fixed-base and compliant base models.

2 ANALYSIS METHODOLOGY

A generic bridge founded on *N* pile groups is considered (Figure 1a). Under the assumption that the non-linear behaviour of the soil-foundation system can be studied through a linear equivalent approach, the SSI problem is handled according to the substructure method, and the kinematic problem is solved in the frequency domain. By assuming that interactions between pile groups supporting different piers are negligible, the soil-foundation system under each bridge support is studied independently, making use of the finite element model proposed by Dezi et al. (2009) for the kinematic interaction analysis of pile groups. For the *i*-th foundation, the following system of complex linear equations, governing the dynamic problem, may be assembled:

$$\left[\begin{array}{c|c}\mathbf{Z}_{CC} & \mathbf{Z}_{CE}\\ \hline \mathbf{Z}_{EC} & \mathbf{Z}_{EE}\end{array}\right]_{F,i}\left[\begin{array}{c}\mathbf{d}_C\\ \hline \mathbf{d}_E\end{array}\right]_i=\left[\begin{array}{c}\mathbf{f}_C\\ \hline \mathbf{f}_E\end{array}\right]_i \quad (1)$$

where **Z** is the dynamic stiffness matrix of the system, **f** is the vector of nodal forces and **d** is the vector of nodal displacements, which are suitably partitioned in order to highlight components of the embedded piles (*E*) and of the rigid cap (*C*) (Figure 1b). According to the adopted model, matrix **Z** accounts for soil-pile and pile-soil-pile interaction, while **f** collects the soil-pile interaction forces arising as a consequence of the seismic soil motion; they are defined as:

$$\left[\begin{array}{c|c}\mathbf{Z}_{CC} & \mathbf{Z}_{CE}\\ \hline \mathbf{Z}_{EC} & \mathbf{Z}_{EE}\end{array}\right]_{F,i}=\mathbf{A}_i^T\left(\mathbf{K}_{P,i}-\omega^2\mathbf{M}_{P,i}+\mathbf{Z}_{P,i}\right)\mathbf{A}_i \quad (2a)$$

$$\left[\begin{array}{c}\mathbf{f}_C\\ \hline \mathbf{f}_E\end{array}\right]_i=\mathbf{A}_i^T\mathbf{Z}_{P,i}\mathbf{d}_{ff,i} \quad (2b)$$

In Equation (2), $\mathbf{K}_{P,i}$ and $\mathbf{M}_{P,i}$ are the frequency-independent stiffness and mass matrices of piles, respectively, $\mathbf{Z}_{P,i}$ is the complex frequency-dependent impedance matrix of the unbounded soil and $\mathbf{d}_{ff,i}$ is the free-field displacement vector within the deposit at the location of the *i*-th foundation.

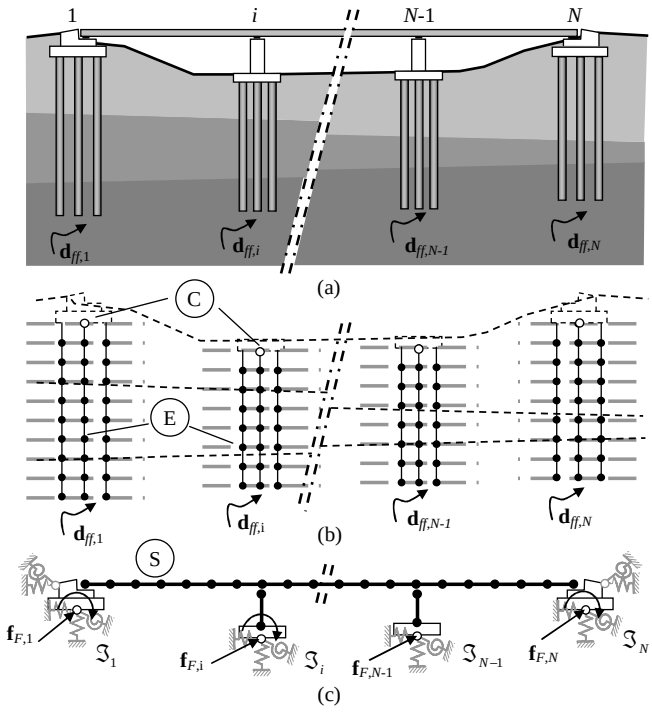

Figure 1. (a) Whole system; (b) model for soil-foundation system, (c) superstructure system.

Being the free-field displacement vector potentially different at each foundation, the approach allows including non-synchronism effects on the bridge, induced by the local soil conditions; these may be captured by performing either independent 1D SV-wave propagation analyses under each support or a unique 2D or 3D seismic response analysis.

Finally, $\boldsymbol{A}_i$ is a geometric matrix representing the kinematic constraint at the head of the *i*-th pile group. By simply manipulating system (1), the soil-foundation impedance matrix $\Im_i$ and the foundation input motion, $\mathbf{d}_C$, necessary to perform inertial soil-structure interaction analysis, may be derived as follows:

$$\Im_i = \mathbf{Z}_{CC,F,i} - \mathbf{Z}_{CE,F,i}\mathbf{Z}_{EE,F,i}^{-1}\mathbf{Z}_{EC,F,i} \tag{3a}$$

$$\mathbf{d}_{C,i} = \Im_i^{-1}\left(\mathbf{f}_{C,i} - \mathbf{Z}_{CE,F,i}\mathbf{Z}_{EE,F,i}^{-1}\mathbf{f}_{C,i}\right) \tag{3b}$$

The inertial interaction analysis is performed in the time domain to reproduce the non-linear behaviour of the superstructure. The frequency-dependent dynamic behaviour of the soil-foundation system is simulated by introducing suitable LPMs with frequency-independent parameters at the base of the superstructure (Wolf, 1994). Impedances of LPMs $\tilde{\Im}_i$ must approximate those of the soil-foundation system $\Im_i$ within the frequency range in which the input motion has the highest energy content and within which the fundamental periods of the structural vibration modes fall; the range 0÷10 Hz is usually considered for this purpose. The dynamic stiffness matrix of the soil foundation system may be re-formulated for the *i*-th pile group as follows:

$$\begin{aligned}\left[\begin{array}{c|c}\mathbf{Z}_{CC} & \mathbf{Z}_{CE}\\ \hline \mathbf{Z}_{EC} & \mathbf{Z}_{EE}\end{array}\right]_{F,i} &\cong \left[\begin{array}{c|c}\mathbf{K}_{CC} & \mathbf{K}_{CH}\\ \hline \mathbf{K}_{HC} & \mathbf{K}_{HH}\end{array}\right]_{LPM,i}\\ -\omega^2\left[\begin{array}{c|c}\mathbf{M}_{CC} & \mathbf{0}\\ \hline \mathbf{0} & \mathbf{M}_{HH}\end{array}\right]_{LPM,i} &+ i\omega\left[\begin{array}{c|c}\mathbf{C}_{CC} & \mathbf{C}_{CH}\\ \hline \mathbf{C}_{HC} & \mathbf{C}_{HH}\end{array}\right]_{LPM,i}\end{aligned} \tag{4}$$

where subscript *H* refers to internal degrees of freedom of the LPM and **K**, **M** and **C** are positive definite matrices with frequency-independent components. The foundation input motion (FIM) is applied at the base of the superstructure by considering forces acting at the caps of pile groups; for the *i*-th group, these forces are transformed in the time domain with the following expression:

$$\mathbf{f}_{F,i}(t) = \frac{1}{2\pi}\int_{-\infty}^{\infty}\tilde{\Im}_i\mathbf{d}_{FIM,i}e^{j\omega t}d\omega \tag{5}$$

The inertial interaction problem of the discrete system (Figure 1c) may be formulated as:

$$\begin{aligned}&\left[\begin{array}{c|c}\mathbf{M}_{SS} & \mathbf{0}\\ \hline \mathbf{0} & \mathbf{M}_{FF}+\mathbf{M}_{LPM}\end{array}\right]\left[\begin{array}{c}\ddot{\mathbf{u}}_S\\ \ddot{\mathbf{u}}_F\end{array}\right]\\ &+\left[\begin{array}{c|c}\mathbf{C}_{SS} & \mathbf{C}_{SF}\\ \hline \mathbf{C}_{FS} & \mathbf{C}_{FF}+\mathbf{C}_{LPM}\end{array}\right]\left[\begin{array}{c}\dot{\mathbf{u}}_S\\ \dot{\mathbf{u}}_F\end{array}\right]+\left[\begin{array}{c|c}\mathbf{0} & \mathbf{0}\\ \hline \mathbf{0} & \mathbf{K}_{LPM}\end{array}\right]\left[\begin{array}{c}\mathbf{u}_S\\ \mathbf{u}_F\end{array}\right]\\ &+\mathbf{f}_{NL}(\mathbf{u},\dot{\mathbf{u}}) = \left[\begin{array}{c}\mathbf{0}\\ \mathbf{f}_F\end{array}\right]\end{aligned} \tag{6}$$

where **M** is the mass matrix of the system, obtained by assembling structural masses ($\mathbf{M}_{SS}$ and $\mathbf{M}_{FF}$ relevant to masses of the deck, piers and foundation caps) and masses of LPMs ($\mathbf{M}_{LPM}$), and **C** is the damping matrix resulting from the relevant contributions of LPMs ($\mathbf{C}_{LPM}$) and of the structure. The latter may be calibrated on the basis of the tangent stiffness matrix, in order to assure a target structural damping (usually 5%). Furthermore, $\mathbf{K}_{LPM}$ is the stiffness matrix obtained by considering contributions of LMPs and $\mathbf{f}_{NL}$ is the vector of the non-linear restoring forces of the system. Finally, $\mathbf{f}_F$ is the vector collecting forces evaluated with Equation (5) by considering the different foundation input motions at each pier.

3 CASE STUDY

The previous procedure is applied to investigate the seismic behaviour of a long multi-span bridge. In particular, the 10-span viaduct (Figure 2) with continuous steel-concrete composite deck reported in Figure 3 is considered.

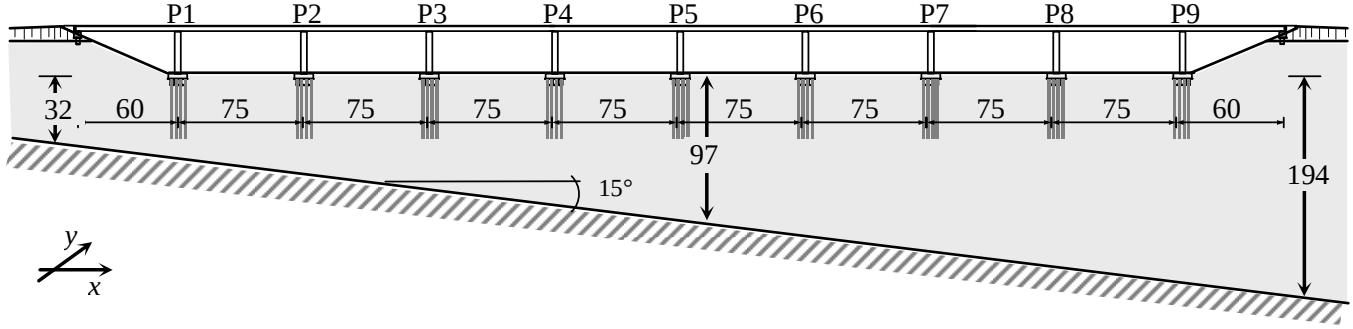

Figure 2. Lateral view of the viaduct.

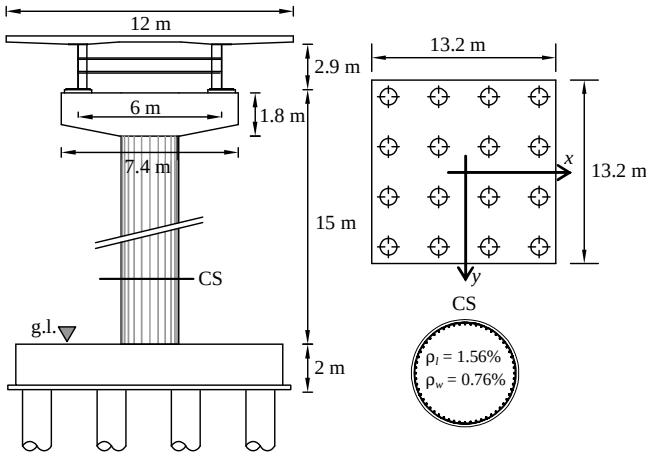

Figure 3. Pier and pile foundation layout.

Table 1. Selected earthquakes

Earthquake	Station	Date
Campano Lucano	Auletta	23/11/80
Lazio Abruzzo	Ponte Corvo	07/05/84
Umbria Marche	Cascia	14/10/97
South Iceland (aftershock)	Flagbjarnarholt	21/06/00
South Iceland (aftershock)	Selfoss-CH	21/06/00
South Iceland	Flagbjarnarholt	17/06/00
Montenegro	Ulcinnj	15/04/79

The bridge has already been object of a previous study aimed at investigate soil-structure interaction effects in the case of uniform soil conditions (Carbonari et al., 2012). Under dynamic loading, the bridge is fixed at all piers (P#) while multi-directional bearings are used in order to avoid a double-path resisting mechanism that would strongly involve the deck. Foundations are constituted by groups of 16 bored r.c. piles with 1.2 m diameter and 30 m long (Figure 3).

For the present application the interface between the superficial soft soil deposit and the seismic bedrock, parallel to the transverse direction of the bridge, is 15° sloped (Figure 2). The deposit is constituted by normally consolidated clays with properties reported in Figure 4a and the variability with depth of the small-strain shear modulus (G_0) is defined according to empirical formulas (d'Onofrio and Silvestri, 2001). The resulting shear wave velocity profile (Figure 4a) corresponds to an equivalent $V_{s,30}$ (149 m/s) falling in the range defined by EN1998-1 for soil class D. The bedrock has shear wave velocity $V_{s,b}$ = 1000 m/s and density ρ_b = 2.0 Mg/m^3.

The seismic design of the bridge follows a direct displacement-based approach, by considering a single pier (SDOF system) clamped at the base. The type I elastic displacement response spectrum defined by EN1998-1 for soil class D is adopted, by considering an amplified Peak Ground Acceleration (PGA) of 0.47g, corresponding to a reference 0.35g in soil type A. The 15 m high circular piers of diameter 2.4 m are designed to withstand the displacement demand with an expected ductility $\mu \approx 2$. The "30%-rule". is used to account for the bi-directional seismic action and the shear failure is prevented by means of a suitable capacity design. Reinforcement ratios (Figure 3) and detailing of structural elements comply with provisions of EN1998-2 (2004). Further details of the bridge design can be found in Carbonari et al. (2012).

3.1 Non Synchronous Seismic Input due to Site Effects

The reference input motion is constituted by a set of seven real records defined at outcropping bedrock and selected so that their mean acceleration elastic response spectrum, normalised with respect to PGA, matches the relevant normalised spectrum suggested by EN1998-1 for soil type A.

The input motions, reported in Table 1, are characterized by 2 orthogonal horizontal components digitalised by free-field stations located on rock outcrop, with magnitude, M_w, ranging between 5 and 7, and epicentral distances, Δ, less than 30 km. The signals are scaled in order to obtain the design hazard level and the mean scale factor adopted is about 4.3.

Independent site response analyses are performed in the *x* and *y* directions to capture stratigraphic amplification effects and to evaluate the non-synchronous seismic motion at the ground surface. In particular, since the soil-bedrock interface is only sloped in the *x* direction, the free field motion along the *y* axis (Figure 2) is evaluated under each support by means of a set of independent 1D site response analyses.

Conversely, stratigraphic amplification effects in the longitudinal direction are quantified by both performing several 1D independent site response analyses in correspondence of each pier and a global 2D non-linear site response analysis of the entire deposit. The aim of this dual approach is essentially the evaluation of the contribution of both soil nonlinearity and bi-dimensional effects on the site response in order to judge the applicability of simplified 1D approaches.

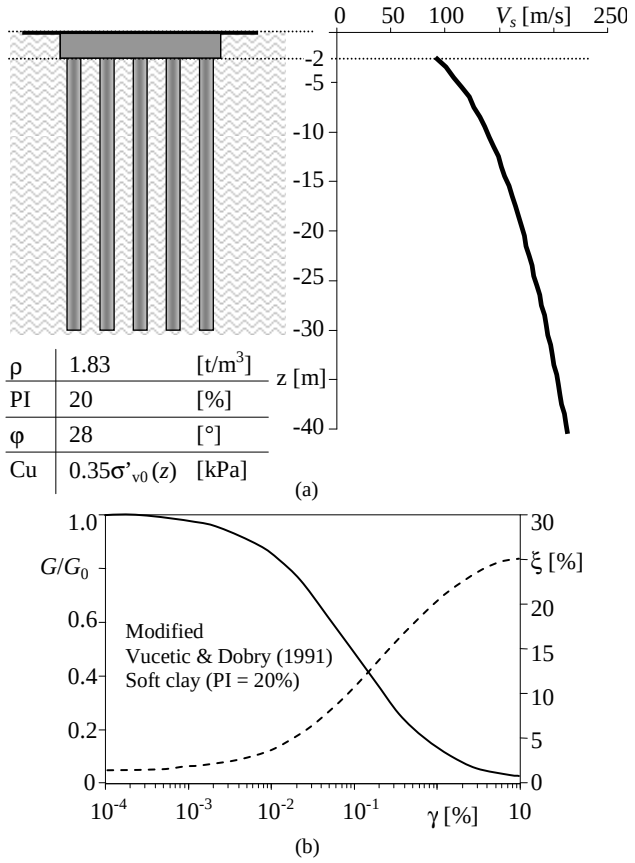

Figure 4. (a) V_s profile and soil mechanical properties; (b) normalized shear modulus and damping ratio curves

For the 1D site response analyses a linear equivalent model in frequency domain formulation is used for the soil, calibrating shear modulus and damping consistently with the maximum strain level attained during the shaking on the basis of standard curves suggested by Vucetic and Dobry (1991), reported in Figure 4b. Due to the high motion amplitude and soil deformability, the maximum shear strain often resulted higher than the volumetric threshold strain equal to 0.05%, indicated by Vucetic (1994) for a typical clay with PI=20%; also, the peak shear stress was sometimes checked to trespass the undrained strength. Nevertheless, the linear 1D approach may be considered conservative since it underestimates energy dissipation due to local soil failure and the aim of the paper is that of evaluating the reliability of simplified 1D approaches with respect to non-linear 2D models.

The free-field response analyses under plane strain conditions (2D) were carried out with the finite difference code FLAC (Itasca, 2011). A simple non-linear visco-elastic perfectly plastic model implemented in a time domain formulation is used for the soil cyclic behaviour according to the soil propriety reported in Figure 4. The geometry and the computation grid are shown in Figure 5. The maximum size of computation mesh elements has been fixed in order to allow the correct propagation of harmonics with a 15 Hz maximum frequency, which is the maximum frequency of the seismic signals adopted in this study, according to the well-known indications by Lysmer and Kuhlemeyer (1973). To minimize reflection effects on vertical lateral boundaries of the grid, free field boundary conditions available in FLAC library have been used.

Figure 6 shows Fourier amplitudes of accelerations obtained from the 2D and 1D models at the ground surface in correspondence of P1, P5 and P9 for 3 of the selected acceleration time histories. Fourier amplitudes obtained from the 2D model are overall greater than those calculated with the 1D model in the $0 \div 10$ Hz frequency range, particularly for pier P1 and P5. Actually, differences between 1D and 2D models attenuate passing from P1 to P9, where hypotheses of 1D propagation appear to be founded. The buried bedrock geometry analysed with the 2D model produces surface waves due to the combination between the inclined refracted SV-waves and P-waves generated by the inclined soil-bedrock surface.

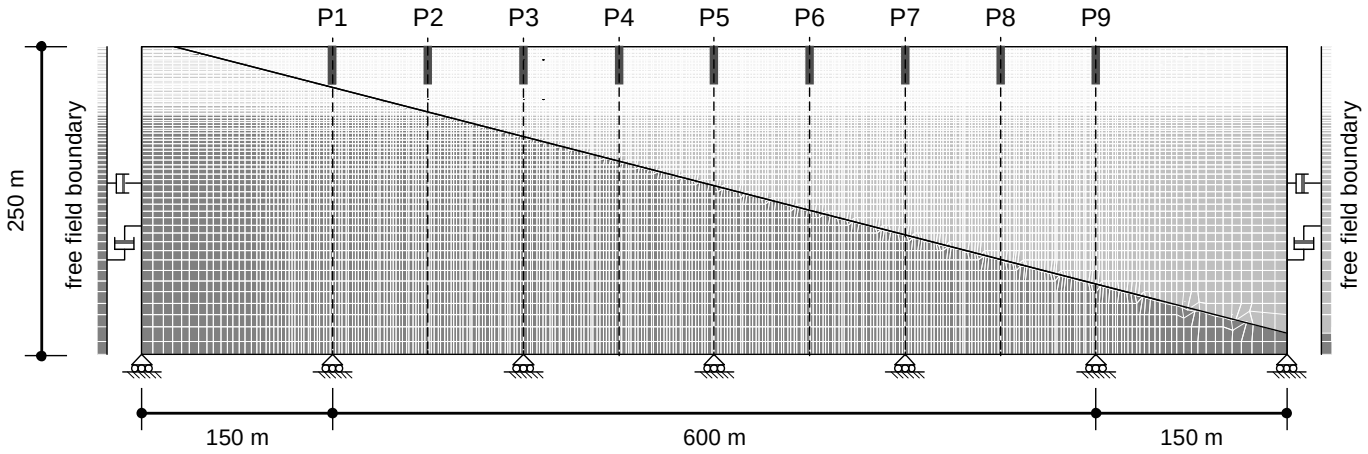

Figure 5. Model geometry and mesh for 2D analyses.

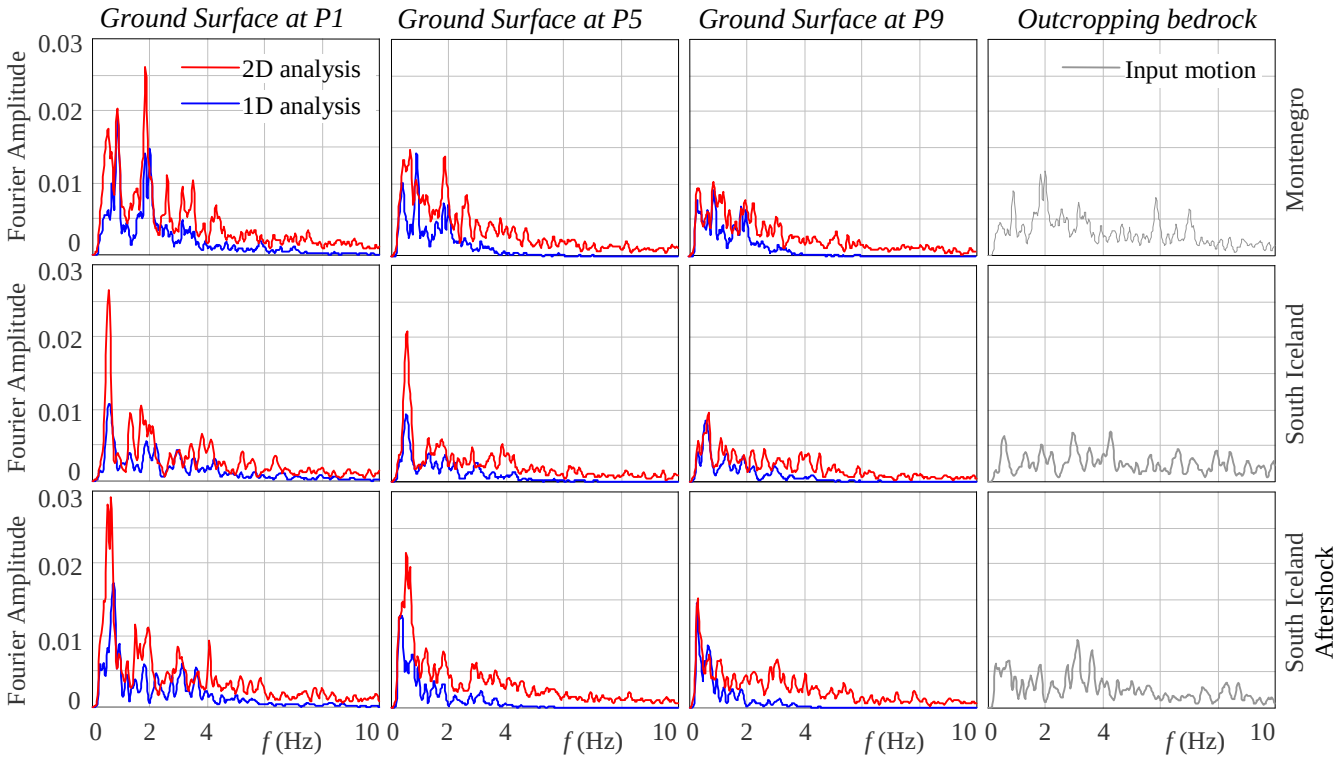

Figure 6. Fourier amplitude of signals at the outcropping bedrock and ground surface obtained from 2D and 1D models at P1, P5 and P9 for 3 earthquakes.

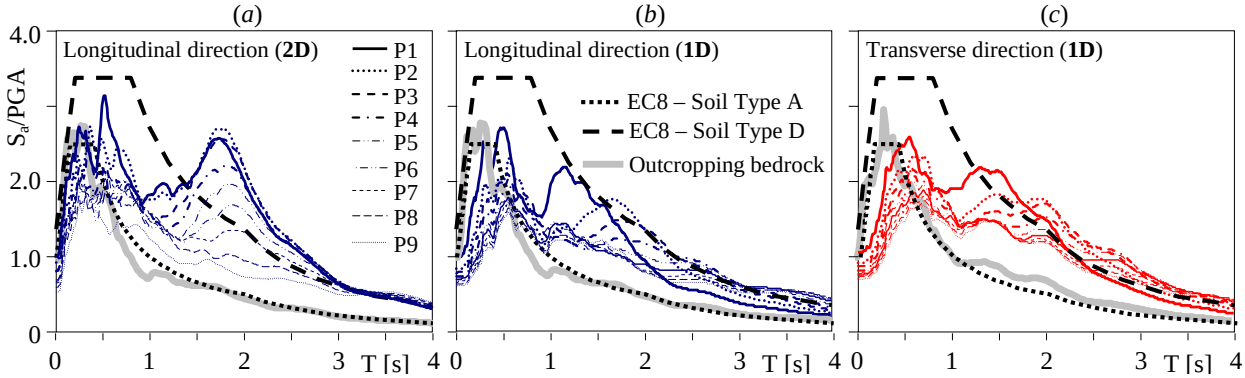

Figure 7. Mean acceleration response spectra of signals at the ground surface under each support for the (a, b) longitudinal direction and (c) transverse direction.

The interaction between surface waves, reflected, and incident wave fields modifies the shaking amplitude that depends on the phase shift of the signals. Both geometrical effects and phase shift are linked to the signal frequency, which is variable according to the non-linear soil behaviour. Motion amplification on surface layer appears more evident for harmonics that interact in phase, approximately in the frequency band 0.4-0.7 Hz, and it decreases with the increasing soil depth. This is due to the verticalization of wave incident fields and to the geometric damping of surface waves.

Figure 7 shows the mean elastic response spectra obtained at the ground surface at the location of each pier obtained for the longitudinal direction, from both the 2D (Figure 7a) and 1D soil models (Figure 7b), and for the transverse direction (Figure 7c). The mean acceleration response spectrum of the selected accelerograms at the outcropping bedrock and the design code spectra for soil type D and A are also reported for comparison.

For what concerns 1D models, spectral amplifications are evident at all piers for periods greater than 1 s and result overall consistent with those quantified by the code; moving from P1 to P9, the period corresponding to the highest amplification increases, as a consequence of the increasing bedrock depth. Focusing on the 2D model, higher spectral ordinates are observed in conjunction with a slight peaks shift towards higher periods; this effect is particularly evident for pier P1.

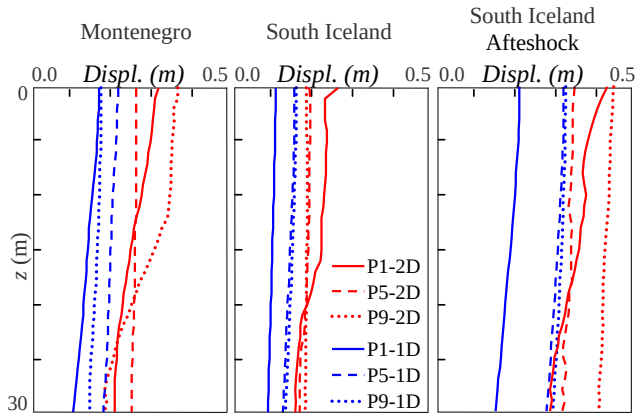

Figure 8. Soil displacement profiles beneath 3 supports for different accelerograms.

Overall, spectral ordinates in the range 1.5 ÷ 3 s are higher than those of the EN1998-1 spectrum for soil type D.

In Figure 8 profiles of the maximum absolute displacements of the first 30 m of soil columns beneath piers P1, P5 and P9 are shown for 3 accelerograms. Displacements obtained from the 2D model are generally greater than those resulting from the 1D analyses; as previously observed, this is due to amplifications induced by the surface waves field that is present in the 2D model.

3.2 Kinematic and Inertial Interaction Analyses

Analyses of the soil-foundation systems are performed with the numerical model proposed by Dezi et al. (2009); piles, modelled with 1 m long beam elements, have density $\rho_p = 2.5$ Mg/m³ and Young's modulus $E_p \approx 23.5$ GPa to account for concrete cracking. Figure 9 shows the translational, rotational and coupled roto-translational components of impedance matrix of the piers foundation. For the sake of simplicity, the small-strain shear modulus is adopted to evaluate the soil-pile impedance so that, according to Dezi et al. (2009), the dynamic stiffness of the soil-foundation system is the same for all the bridge supports. Non-linear inertial interaction analyses are carried out in time domain, developing a 3D finite element model of the bridge. Linear elastic beam elements are used for the deck, while fiber elements are adopted for piers to capture their non-linear behaviour under bidirectional excitation. Cross-section properties of members are based on the suggestions by Mander et al. (1988) for confined and unconfined concrete and by Menegotto and Pinto (1973) for rebars. Furthermore, 5% structural damping is introduced in terms of tangent stiffness proportional damping. Both Compliant Base (CB) and Fixed-Base (FB) models are developed in order to investigate the contribution of SSI in the structural response.

With reference to CB models, Figure 10 depicts the LPMs used to represent the frequency dependent behaviour of the soil-foundation system in the inertial interaction analysis (Carbonari et al., 2012); they are calibrated to reproduce the impedance functions of the actual soil-foundation system in the frequency range 0÷10 Hz (Figure 9). Besides, the Foundation Input Motions are represented by generalised forces applied at the level of each pile caps. Due to the inclined configuration of the soil-bedrock interface, the seismic actions are different at each pier and account for the site-induced non-synchronism.

For the FB models, input actions are constituted directly by accelerations evaluated at the ground surface, in correspondence of each bridge pier; even in this case seismic actions account for the non-synchronism induced by site effects.

3.3 Main Results

The effects of the spatial variability of ground motion due to site effects on the non-linear seismic response of the bridge are addressed in this section, in terms of piers displacement and ductility demands.

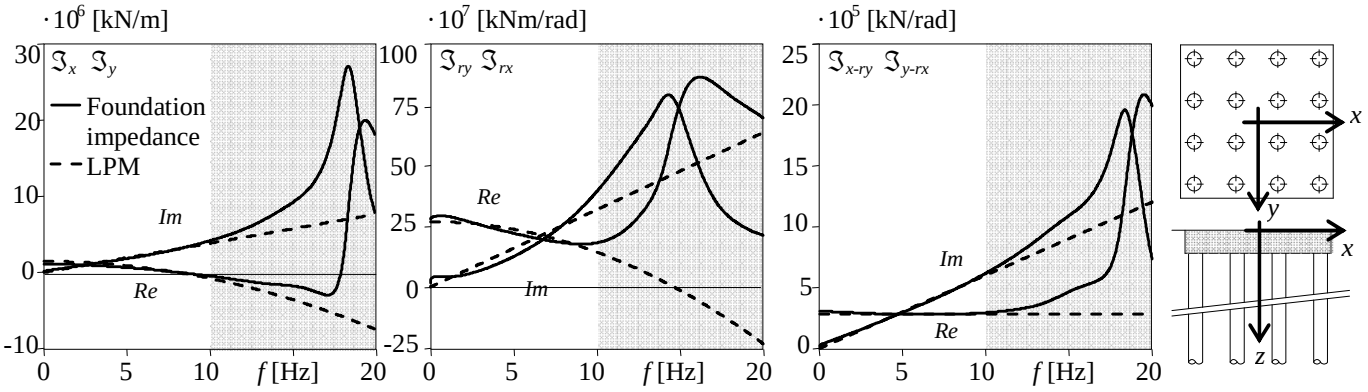

Figure 9. Components of the soil-foundation system impedance matrix.

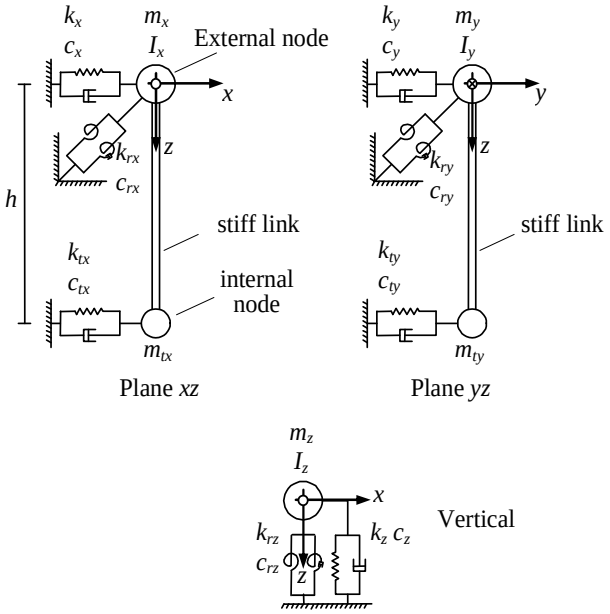

Figure 10. Adopted LMP

Differences resulting from the use of the 1D and 2D models to describe the free field behaviour are evaluated, quantifying approximations introduced by the more simplified approach. In addition, the role of SSI on the structural response of the bridge is illustrated comparing results of FB and CB models.

Results are presented in terms of mean values obtained from inertial analyses performed with all the accelerograms.

Figure 11a shows the maximum absolute values of the combined (*x*-*y*) relative displacements of piers head obtained for the FB and CB models by considering the non-synchronous motions resulting from 1D and 2D soil models. Displacements are evaluated with respect to the foundation and include both the plastic and elastic pier deflection as well as the contribution due to the foundation rocking. The use of simplified 1D soil models in correspondence of each pear for the definition of the non-synchronous action for the bridge leads to underestimate the piers displacements, for both the FB and CB models. In addition, for FB models discrepancies between results relevant to 1D and 2D soil models are almost constant for all piers while for CB models discrepancies are less pronounced for central piers (P4, P5 and P6). Overall, the increment of the displacement demand is consistent with considerations provided in previous sections, relevant to higher amplifications induced by the 2D nonlinear soil model on the seismic motion.

Figure 11b and c show the rotational demand of plastic hinges at the piers base and the displacement ductility demand of piers, evaluated with reference to the combined bidirectional motion, by suitably accounting for the effects of the foundation rigid rotation; results obtained considering the site response provided by the 1D and 2D models for the soil are plotted, for both FB and CB models. As expected, previous considerations on displacements hold: with reference to Figure 11b, for both FB and CB structures, the use of the 1D model for the soil leads to underestimate sensibly the rotation demand of plastic hinges at lateral piers (P1, P2, P3, P7, P8 and P9) while for central piers (P4, P5 and P6) the underestimation is less important.

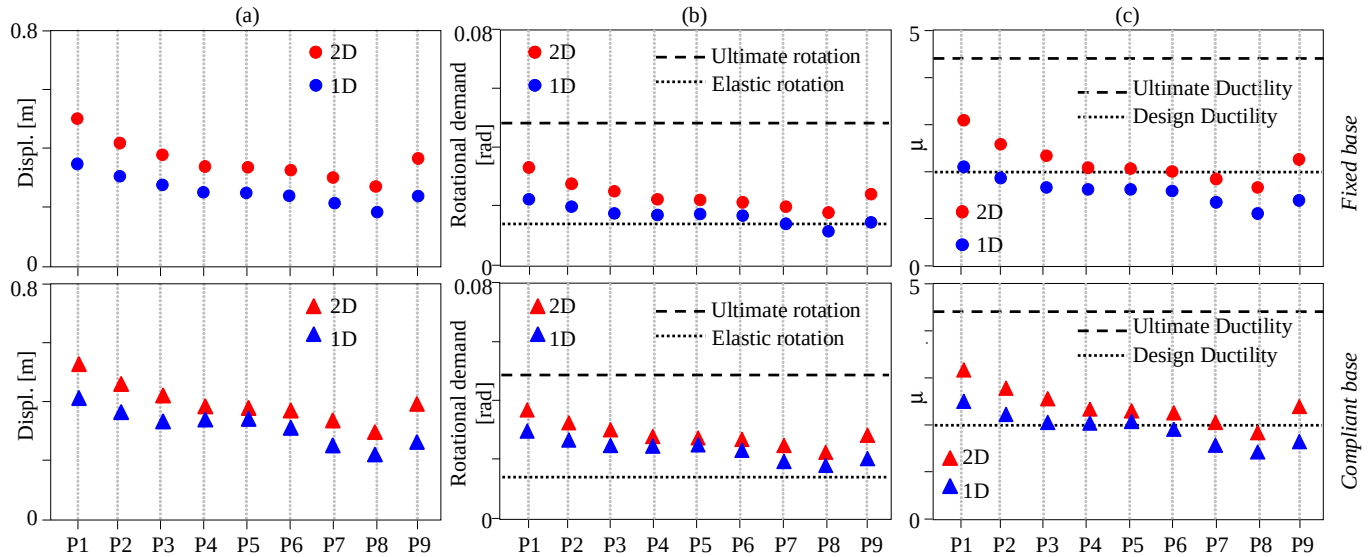

Figure 11. For both FB and CB models: (a) absolute values of maximum piers relative displacement; (b) rotational demand of plastic hinges at piers base; (c) ductility demand of piers.

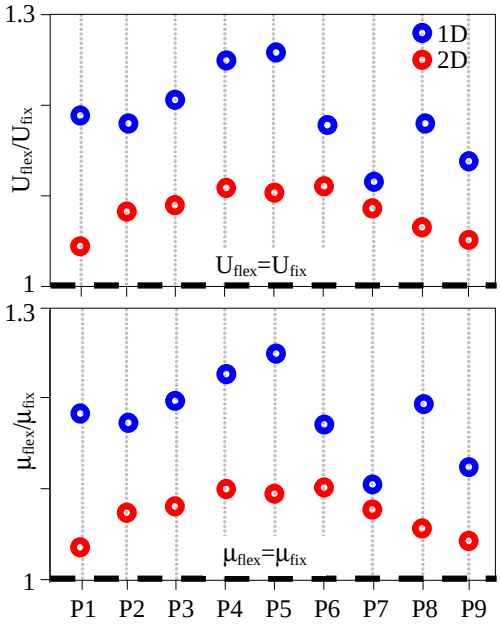

Figure 12. Ratio of response quantities obtained from CB and FB models.

Furthermore, for all cases investigated, the piers ductility demand (Figure 11c) is almost the same for central piers and is close to the design value, while for lateral piers greater or lower values than the design one are observed. Overall, the ductility demand increases as a consequence of the SSI.

In order to quantify the contribution of SSI on the bridge response under non-synchronous actions, the ratio of response quantities obtained from CB and FB models are evaluated. Figure 12a and b shows these ratios for the piers displacements and for the piers ductility demand.

Ratios are greater than 1 for all piers, meaning that SSI always produces an increment of the demand parameters. In addition increments resulting from the use of the non-synchronous actions from 1D soil models are within the range 10÷25% and appear sensibly higher that those computed by using actions from the 2D model (included in the range 5÷10%).

4 CONCLUSIONS

A numerical methodology, based on the domain decomposition technique, has been presented and adopted to study effects of non-synchronous seismic motion induced by local stratigraphic conditions in the SSI analysis of multi-span viaducts on pile foundations. The methodology may be applied once the free-field motion within the deposit is determined; results from 1D, 2D or 3D models, depending on the deposit complexity, may be used to this purpose.

A case study constituted by a multi-span bridge founded on a soft clay deposit overlaying an inclined bedrock is considered and the seismic action is represented by real accelerograms defined at the outcropping bedrock. The spatial variation of ground motion for the bridge is evaluated by adopting different seismic ground response models in order to quantify approximations involved in the use of simplified approaches. The structural responses obtained starting from the different ground response approach for the evaluation of the non-synchronous action are compared, also discussing the significance of SSI effects. The following main conclusions may be drawn:

- spectral amplifications of accelerations at the ground surface resulting from the 2D models are overall higher than those obtained from monodimensional propagation analyses. Nonetheless, discrepancies between results of the two models attenuate by increasing the bedrock depth due to the gradual attenuation of the 2D effects which are focused near the edge of the deposit where the inclination of the refracted waves generates surface waves;
- the structural demand parameters (e.g. pier displacements and ductility) obtained adopting the non synchronous actions from the 2D model are sensibly higher than those obtained using actions derived from the 1D soil model;
- SSI always produces an increment of the demand parameters; these are more significant (10÷25%) if the seismic action derives from 1D soil model.

Applications demonstrate that the use of simplified 1D linear equivalent propagation models to capture stratigraphic amplification effects in the case of 2D deposit configurations may lead to underestimate sensibly the free-field motion, especially in the case of soft soils and high seismic intensities. In such situations 2D nonlinear soil models should be preferred to capture the actual wave field near the ground surface, strongly affected by superficial waves, and to obtain a reliable prediction of soil displacements. The structural response obtained by considering seismic inputs derived from 1D or 2D soil models can differ sensibly; in any SSI always plays a significant role in the structural response of bridges.

REFERENCES

Abrahamson NA, Schneider JF, Stepp JC, 1991. Empirical spatial coherency functions for application to soil-structure to soil-structure interaction analyses, *Earthq. Spectra*, **7**(2), 1-27.

Carbonari S, Dezi F, Leoni G, 2011. Seismic soil-structure interaction in multi-span bridges: application to a railway bridge, *Earthq. Eng. & Struct. Dyn*; **40** (11), 1219-1239.

Carbonari S, Morici M, Dezi F, Nuti C, Silvestri F, Tropeano G, Vanzi I, 2012. Seismic response of viaducts accounting for soil-structure interaction, *15 WCEE*, Sept. 2012, Lisbon, Portugal.

Dezi, F, Carbonari S, Leoni G, 2009. A model for the 3D kinematic interaction analysis of pile groups in layered soils, *Earthquake Engng Struct. Dyn.*, **38**(11), 1281–1305.

d'Onofrio A, Silvestri F., 2001. Influence of micro-structure on small-strain stiffness and damping of fine grained soils and effects on local site response. *IV Int. Conf. on 'Recent Advances in Geotech*. *Earthquake Engng and Soil Dynamics*'. S. Diego, CA.

EN 1998-1, 2004 Eurocode 8: Design of structures for earthquake resistance - Part 1: General rules, seismic actions and rules for buildings.

EN 1998-2, 2004 Eurocode 8: Design of structures for earthquake resistance - Part 2: Bridges.

Itasca Consulting Group Inc, 2011. Fast Lagrangian Analysis of Continua. User's Guide. 5th Edition (FLAC Version 7.0).

Lupoi A, Franchin P, Monti G, Pinto PE, 2005. Seismic design of bridges accounting for spatial variability of ground motion. *Earthq. Eng. & Struct. Dyn*., **34**, 327-348.

Lysmer J, Kuhlemeyer RL, 1973. Finite Element Method accuracy for wave propagation problems. *Journal of Soil Mechanics & Foundations Division*, ASCE, **99**(SM5), 421-427.

Mander JB, Priestley MJN, Park R, 1988. Theoretical Stress-Strain Model for Confined Concrete. *Journal of Structural Engineering*, **114** (8), 1804-826.

Menegotto M, Pinto PE, 1973. Method of analysis for cyclically loaded R.C. plane frames including changes in geometry and non-elastic behaviour of elements under combined normal force and bending. *Symp. on the resistance and ultimate deformability of structures acted on by well defined repeated loads*, Zurich, Switzerland, 15-22.

Monti G, Nuti C, Pinto PE, 1996. Nonlinear response of bridges under multisupport excitation. *ASCE Jnl Struct. Eng*., **122**(10), 1147-1159.

Sextos AG, Pitilakis KD, Kappos AJ, 2003. Inelastic dynamic analysis of RC bridges accounting for spatial variability of ground motion, site effects and soil-structure interaction phenomena. Part 2: Parametric study. *Earthquake Engng Struct. Dyn.*, **32**(4), 629-52.

Vucetic M, Dobry R, 1991. Effect of soil plasticity on cyclic response. *Journ. of Geot. Eng. ASCE*,; **117**(1), 89-107.

Vucetic M. Cyclic threshold shear strains in soils. *Journal of Geot. Eng. ASCE*, 1994, **120** (12), 2208-2228.

Wolf JP, 1994. Foundation Vibration Analysis Using Simple Physical Models, Prentice-Hall: Englewood Cliffs N.J.